ACS Chemical Neuroscience

Research Article

pubs.acs.org/chemneuro

A Novel Electrochemical Approach for Prolonged Measurement of Absolute Levels of Extracellular Dopamine in Brain Slices

Mark H. Burrell,[†] Christopher W. Atcherley,[‡,§] Michael L. Heien,[‡] and Janusz Lipski*[,†]

[†]Department of Physiology and Centre for Brain Research, Faculty of Medical and Health Sciences, University of Auckland, Auckland 1142, New Zealand

[‡]Department of Chemistry and Biochemistry, University of Arizona, Tucson, Arizona 85721, United States

ABSTRACT: Tonic dopamine (DA) levels influence the activity of dopaminergic neurons and the dynamics of fast dopaminergic transmission. Although carbon fiber microelectrodes and fast-scan cyclic voltammetry (FSCV) have been extensively used to quantify stimulus-induced release and uptake of DA in vivo and in vitro, this technique relies on background subtraction and thus cannot provide information about absolute extracellular concentrations. It is also generally not suitable for prolonged (>90 s) recordings due to drift of the background current. A recently reported, modified FSCV approach called fast-scan controlled-adsorption voltammetry (FSCAV) has been used to assess tonic DA levels in solution and in the anesthetized mouse brain. Here we describe a novel extension of FSCAV to investigate pharmacologically induced, slowly occurring changes in tonic (background) extracellular DA concentration, and phasic (stimulated) DA release in brain slices. FSCAV was used to measure adsorption dynamics and changes in DA concentration (for up to 1.5 h, sampling interval 30 s, detection threshold < 10 nM) evoked by drugs affecting DA release and uptake (amphetamine, L-DOPA, pargyline, cocaine, Ro4-1284) in submerged striatal slices obtained from rats. We also show that combined FSCAV-FSCV recordings can be used for concurrent study of stimulated release and changes in tonic DA concentration. Our results demonstrate that FSCAV can be effectively used in brain slices to measure prolonged changes in extracellular level of endogenous DA expressed as absolute values, complementing studies conducted in vivo with microdialysis.

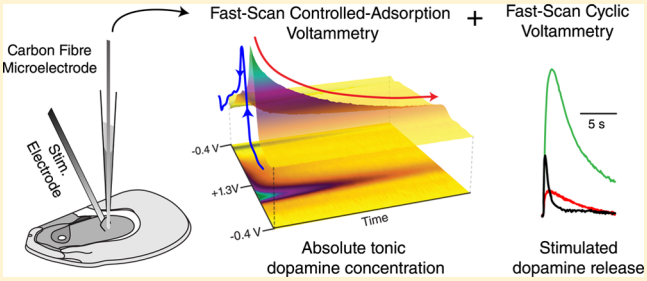

KEYWORDS: *Electrochemistry, dopamine, carbon-fiber microelectrodes, striatum, rat, in vitro*

1. INTRODUCTION

The complex interplay of fast (phasic) and slow (tonic) actions engenders dopamine (DA) with a vast array of functions.[1−3] The fast actions of DA have been extensively studied, both in vivo and in brain slices, with fast-scan cyclic voltammetry (FSCV[4−7]). However, the slow changes in extracellular neurotransmitter concentration cannot be captured with this technique, as it requires subtraction of a background current that is typically unstable during prolonged (>90 s) recordings.[8] Instead, such measurements are usually performed in vivo using microdialysis or push-pull cannula combined with sensitive chromatographic detection (e.g., HPLC[9−11]).

Brain slices, although reductionistic, maintain many key aspects of in vivo biology including intact local brain architecture and synaptic connectivity, and offer certain advantages over studies conducted in vivo (e.g., easier control of the extracellular chemical composition[12]). However, early attempts to investigate tonic DA activity in slices using the radioactive superfusion technique (after preincubation with [^{3}H]DA or [^{3}H] tyrosine[13−15]) have had limited success due to low time resolution and inability to measure absolute values of extracellular DA concentration. Moreover, the low superfusion rates required in such studies (<0.5 mL/min) likely resulted in tissue hypoxia. Conventional microdialysis is not possible in brain slices due to the large size of probes, and while an adaptation of this technique, involving placement of a horizontally oriented microdialysis assembly on the surface of a slice, partly overcame the issue of high dilution seen in superfusion studies, in vitro microdialysis suffers from poor temporal resolution and absolute quantification remains challenging[16] (see also ref 17).

Fast-scan controlled-adsorption voltammetry (FSCAV) is a novel electrochemical technique that adapts the principles and technology of FSCV to measure absolute neurotransmitter concentrations.[18] Developed and validated in silico and in calibration solutions, this technique, like FSCV, uses triangular scans from −0.4 to +1.3 V to measure Faradaic currents of electroactive species, including DA. In doing so, FSCAV generates a cyclic voltammogram, which (like in FSCV) is useful for analyte identification. The fundamental difference between FSCAV and FSCV is that for FSCAV the adsorption of the analyte to the carbon fiber microelectrode (CFM) surface is varied by changing the time between scans. In doing so, FSCAV can reveal information on local diffusion kinetics

Received: April 20, 2015
Revised: August 28, 2015
Published: August 31, 2015

DOI: 10.1021/acschemneuro.5b00120
ACS Chem. Neurosci. 2015, 6, 1802−1812

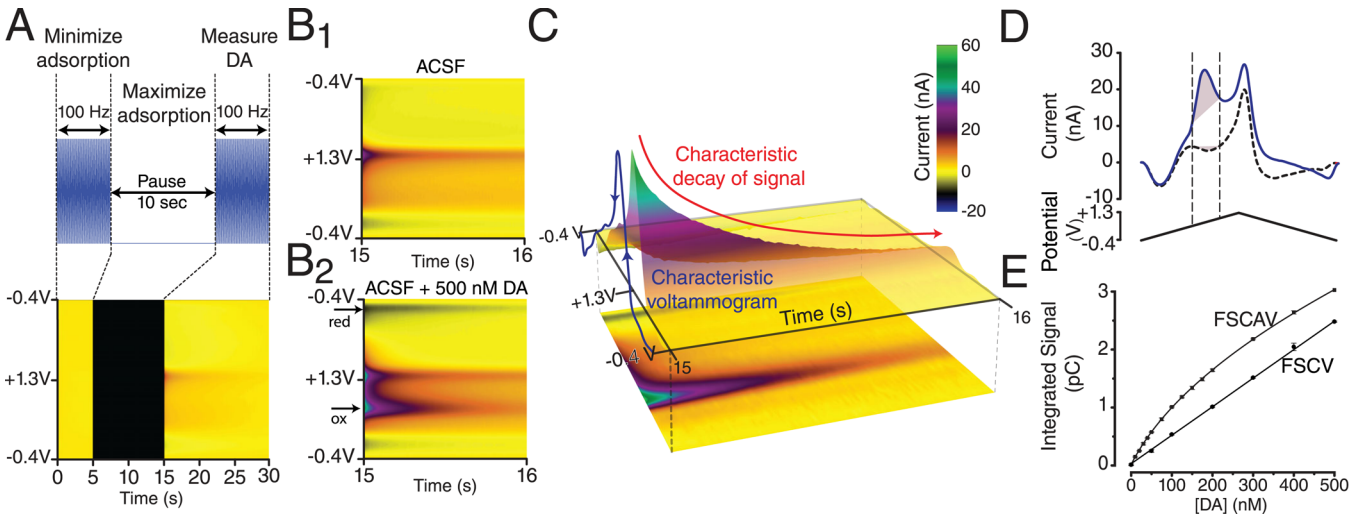

Figure 1. Mechanics of FSCAV. (A) Typical 30 s recording segment consists of 5 s scanning at 100 Hz to minimize adsorption to the electrode, 10 s "pause" during which the electrode is held at −0.4 V to maximize adsorption, and 15 s scanning at 100 Hz. (B) DA concentration is established during the period immediately after the pause (100 ms, 10th scan). DA-dependent and nonspecific changes occur in the current measured postpause, compared to current before the pause. Deconvolution of response in ACSF only (B1) with response in ACSF containing DA (B2) isolates DA-specific changes (oxidation and reduction currents indicated). (C) 3-D representation and 2-D projection of deconvoluted data from (B). Analytes identified by the characteristic voltammogram (as in FSCV) and rate of decay of the Faradaic current. (D) Integrating a limited portion of the raw (not deconvoluted) 10th scan postpause (between +0.4 and +0.9 V; shaded) allows quantification of DA concentration (solid line, 500 nM DA; dotted line, ACSF only). (E) This integrated signal (the "FSCAV signal") correlates with absolute DA concentration (R^2 = 0.99, quadratic model) and is more sensitive than equivalent signal recorded with FSCV (10 Hz, 1200 V/s), with concentrations as low as 10 nM still readily detectable (n = 3 each point, single CFM).

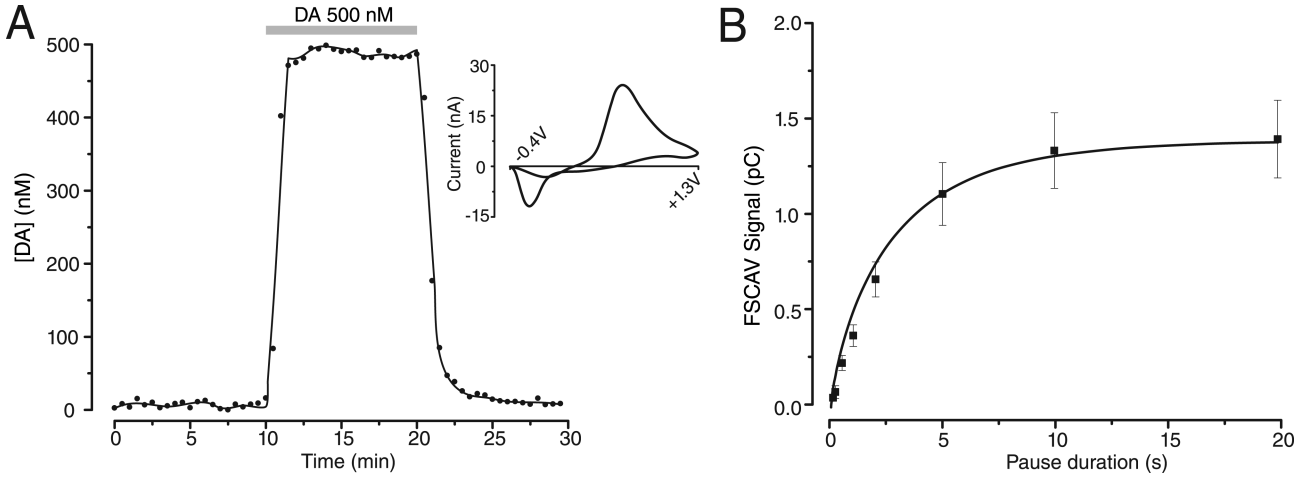

Figure 2. Detection of DA outside and inside the striatal slice with FSCAV. (A) Example of a prolonged measurement of DA concentration in the recording chamber with a CFM positioned above the slice during exogenous DA application (500 nM) for 10 min. Measured DA concentration: 489 ± 5 nM. Inset: Deconvoluted voltammogram from measurement during DA application, demonstrating characteristic oxidation and reduction peaks. (B) Varying pause length (controlled adsorption period) reveals mass transport kinetics of DA in slice when extracellular DA concentration was enhanced. Fitting of a previously validated finite-difference simulation was used to determine the diffusion coefficient of DA in slice (4.75 ± 0.46 × 10^{-6} cm^2 s^{-1}; n = 6).

and the absolute concentration of such analytes. This approach has already been used to measure baseline and drug-induced tonic levels of extracellular DA concentration in the intact mouse brain.[19]

We have now adopted FSCAV to measure adsorption dynamics and tonic levels of extracellular DA concentration (in recordings lasting for up to 1.5 h) evoked by drugs affecting DA release and uptake in submerged rat brain slices containing the striatum. We also show that combined FSCAV-FSCV recordings, performed on one CFM, allow concurrent study of electrically stimulated release and changes in the absolute tonic concentrations of DA. Our data demonstrate that FSCAV can be effectively used to measure slow changes in extracellular levels of endogenous DA in brain slices, complementing neurotransmitter release studies conducted in vivo with other electrochemical techniques and microdialysis.

2. RESULTS AND DISCUSSION

2.1. General Principle of FSCAV. The general mechanics of FSCAV are presented in Figure 1, based on the optimal parameters established by Atcherley et al.:[18] In each 30 s recording segment, the triangular voltage scans are first applied

DOI: 10.1021/acschemneuro.5b00120
ACS Chem. Neurosci. 2015, 6, 1802−1812

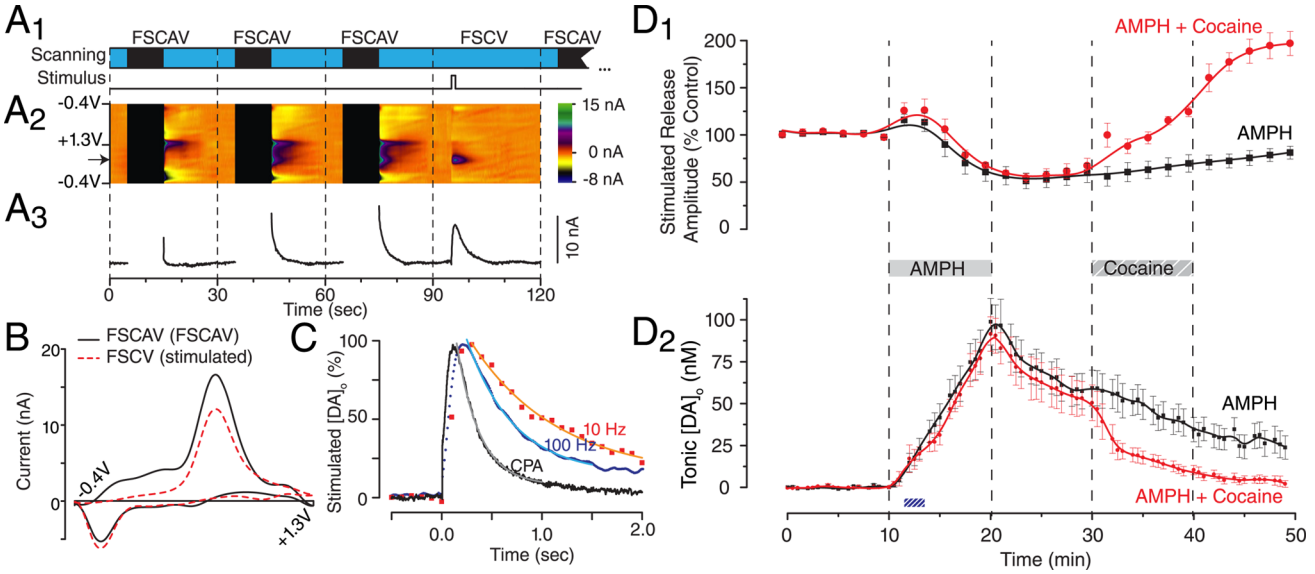

Figure 3. Combined FSCAV-FSCV recordings showing effects of amphetamine (AMPH) on tonic DA and stimulated release. (A) FSCAV-FSCV recording paradigm conducted during time indicated by hatched blue bar in (D). FSCV recording segments, in which an electrical stimulus is applied and 100 Hz scanning (blue) is uninterrupted, are interposed between FSCAV measurements (A1). Pauses of scanning used for FSCAV marked in black. As DA concentration increases, greater postpause Faradaic current was observed at ~0.7 V (arrow; color-plot in A2, current in A3) in successive FSCAV recording segments. FSCAV signal was calibrated to estimate tonic $[DA]_0$; the amplitude of stimulated release was used to quantify evoked release. (B) Oxidation and reduction peaks are similar in deconvoluted FSCAV and stimulated release (FSCV) voltammograms. (C) Release was measured, at the same location, with constant potential amperometry (CPA) and with FSCV conducted at 10 or 100 Hz (both at 1200 V/sec). Apparent rate of reuptake was significantly different for each method. (D) Changes in stimulated release (D1) and tonic DA (D2) following brief application of AMPH (10 μM, n = 6). AMPH transiently increased, then decreased, electrically stimulated DA overflow. AMPH increased tonic DA concentrations. The DAT inhibitor cocaine (20 μM, 10 min, n = 7) accelerated the reduction in tonic DA 10 min following washout of AMPH.

to the CFM at 100 Hz for 5 s to minimize the surface concentration of DA. The electrode is then maintained at −0.4 V for (normally) 10 s. Following this pause (referred to as a "delay time" by Atcherley and co-workers[18,19]), scanning resumes for a further 15 s (Figure 1A). During the pause in scanning, the electrode surface and local concentrations of DA equilibrate, and thus the scans that directly follow can be used to establish absolute DA concentration. Analysis of the color plot of the 1 s period after the pause, before and after adding 500 nM DA to Tris-buffered ACSF, shows Faradaic currents caused by DA oxidation and reduction (Figure 1B2, arrows). The oxidation current can be isolated from changes in the background current resulting from the pause (e.g., the artifact evident at +1.3 V in ACSF only, Figure 1B1) by generating a response function from ACSF only recording, and using this response function to deconvolute the response recorded in ACSF containing DA (see Methods, section 3.3).

DA can be identified by its characteristic voltammogram and a relatively slow (vs L-DOPA and DA metabolites; see section 2.4) rate of decay of the Faradaic current after pause (Figure 1C). However, due to differences between ACSF and the internal environment of the slice, deconvolution is less successful in removing the changes in background current from pausing in slices. Instead, integrating a limited portion of the voltammogram (+0.4 to +0.9 V) of the 10-th scan after each pause gives a charge (measured in picocoulombs, pC) that is closely related to the absolute DA concentration over the nanomolar range and can be used to calibrate measurements in brain slice with signals recorded in buffer, without need for further correction (Figure 1D, E).[19] As discussed previously by Atcherley et al., FSCAV is more sensitive than FSCV over the nanomolar range (Figure 1E).[18] Deconvolution remains the only method for recovering analyte-specific voltammograms, which are useful for species identification and comparison against voltammograms of analytes released by electrical stimulation.

2.2. Detection of Exogenously Applied DA. To confirm FSCAV can track the absolute concentration of DA over a prolonged period of time, 500 nM DA was applied to the recording bath for 10 min. With the CFM placed just above the surface of the slice, the measured DA was 489 ± 5 nM with rapid wash-in and wash-out times (Figure 2A). As DA concentration was sampled every 30 s, the time resolution is clearly superior to that offered by microdialysis (typically 1 data point every 10−20 min). When the electrode was placed in the dorsal striatum ~150 μm below the slice surface, the concentration of DA detected was significantly lower (data not shown), as previously noted with other voltammetric techniques.[20,21]

Within the slice, a small signal was detectable in the absence of exogenous DA (or any drug) between the +0.4 and +0.9 V integration limits, which corresponds to a DA concentration of 11 nM (SD: 13 nM). This signal was present both in the striatum (dopaminergic fiber-rich region) and in the overlaying cerebral cortex (with much lower density of dopaminergic fibers), and was not enhanced by MAO inhibition (see Figure 5). Such small quantities may reflect DA that has lastingly adsorbed to the CFM, rather than DA sampled from the tissue. Thus, in line with the notion that extracellular DA concentration in striatal slice is zero,[5,22] the signal prior to administration of exogenous DA or any pharmacological agent was subtracted from all recordings.

In these measurements, the duration of the pause in scanning in each 30 s recording segment was set as 10 s, based on the assumption that this period is sufficient for reaching equilibrium between the DA in the solution/tissue and that

DOI: 10.1021/acschemneuro.5b00120
ACS Chem. Neurosci. 2015, 6, 1802−1812

adsorbed to the CFM.[18] However, by varying the pause duration (between 0.1 and 20 s) the exact diffusion kinetics of DA can be investigated and this assumption validated, as previously done in beaker and in vivo.[18,19] The principle of this model is that following the local elimination of DA at the electrode during 100 Hz scanning, DA reaches the carbon fiber surface at a rate proportional to the speed of its diffusion in the local environment of the CFM. Thus, measuring DA concentration at the electrode surface after various pause times reveals information about speed of diffusion, as reflected by the diffusion coefficient. An example of such measurement, conducted ~150 μm beneath the slice surface while endogenous DA concentration was pharmacologically enhanced (see section 2.5) is shown in Figure 2B. By fitting this data with the COSMOL model described and validated previously,[18] an estimate of the diffusion coefficient was obtained ($4.75 \pm 0.46 \times 10^{-6}$ cm^2 s^{-1}, n = 6). This coefficient may be used, for example, to assess the degree of edema common with slices kept in CO_2/bicarbonate-buffered ACSF.[23]

2.3. Combined FSCAV and FSCV Analysis of DA Released by Amphetamine. Regular switching between periods of FSCAV, during which measurements of absolute DA concentration are made, and periods of FSCV during which stimulated DA release is detected, allows study of pharmacologically induced, slowly developing (referred to here as "tonic") changes in extracellular DA concentration in parallel with changes in electrically stimulated (referred to as "stimulated release") DA levels. In this way, in each consecutive 2 min period, three measurements of tonic levels with FSCAV and one measurement of stimulated release with FSCV are made (Figure 3A). Stimulated DA release was evoked by a single electrical pulse within the slice. Lowering scanning frequency during FSCV recording of stimulated release (e.g., from 100 to 10 Hz; cf. previous in vivo study[19]) necessitates a period of restabilization of the electrode, but if frequency is maintained at 100 Hz as in the current study, there is no need to stop recording. Thus, the temporal resolution of tonic DA measurement can be largely preserved. The trade-off of using 100 Hz scanning is a lower sensitivity due to the decreased time for DA to adsorb to CFM. However, as compared with conventional FSCV (400 V/s, 10 Hz), stimulated release is still readily detectable with FSCV performed at 100 Hz, attributable to a very high scanning rate[24] (in our case 1200 V/s). The use of scanning frequencies >10 Hz (and higher scanning rates) for FSCV has already been advocated by Kile et al.,[25] as 10 Hz scans may underestimate the rate of release and uptake following electrical stimulation. A temporal lag results from the relatively long periods between scans (100 ms), during which DA is adsorbed to the electrode but not oxidized.[24,26] With an estimate of the DA adsorption kinetics, which can be obtained with FSCAV, this delay can be mathematically removed.[26,27] However, FSCV performed at faster scanning frequencies decreases the need for such correction by shortening the time between adsorption and detection. Kile et al.[25] determined that scanning at high frequency (60 Hz) improves temporal fidelity, closer to the temporal characteristics of constant potential amperometry (CPA). CPA, however, likely overestimates DA uptake as detection is a consumptive process.[6,25] This methodological dependence of the estimate of time-course is evident in our measurements (Figure 3C; CPA, $\tau = 0.14 \pm 0.01$ s; FSCV at 100 Hz, $\tau = 0.33 \pm 0.03$ s; FSCV at 10 Hz, $\tau = 0.59 \pm 0.06$ s; $n = 3$ each). Unlike CPA, 100 Hz FSCV allows analyte identification from the "signature" of the cyclic voltammogram (Figure 3B).

To compare between the FSCAV-FSCV paradigm used here and the FSCV-only approach used in previous studies, we investigated both changes in tonic DA levels (with FSCAV) and stimulated DA release (with FSCV) following application of amphetamine (AMPH). AMPH releases DA by displacing this neurotransmitter from vesicles into the cytosol and then to the extracellular space via DAT.[28] Brief application of AMPH (10 min, 10 μM) slowly increased tonic DA concentration to a peak of 99 ± 12 nM (Figure 3D2; cf. refs 29 and 30). DA concentration remained elevated above baseline for the remainder of the recording period (30 min). AMPH initially increased the amplitude of stimulated DA release (cf. ref 30), consistent with a primary effect of competing with DA at DAT at low concentrations[31] and the relatively slow displacement of DA from vesicles.[29] AMPH subsequently decreased the amplitude of stimulated DA release, likely reflecting the depletion of vesicular DA (cf. refs 29−31).

To illustrate the effectiveness of our FSCAV approach for making sensitive measurement of extracellular DA concentration and to demonstrate the involvement of DAT in prolonged increase in concentration of this neurotransmitter after AMPH, the DAT inhibitor cocaine (20 μM) was added 10 min post AMPH washout. This suddenly and markedly reduced tonic DA concentration, with a 40 ± 8 nM decrease during the 10 min period of cocaine administration ($n = 6$). Without cocaine there was only a 20 ± 2 nM drop in the same time period, ($n = 7$; $p < 0.001$ repeated-measures ANOVA), consistent with previous studies showing that AMPH-induced increases in tonic DA concentration depends on reverse transport through DAT.[28,29] Meanwhile, the amplitude of stimulated DA release was increased by cocaine, reflecting reduced reuptake (Figure 3D1). These experiments show that FSCAV provides an effective way for measuring small changes in the tonic extracellular DA concentration over prolonged periods of time, while still allowing FSCV to be used intermittently to assess changes in stimulated release.

2.4. Combined FSCAV and FSCV Analysis of DA Released after L-DOPA. In comparison to AMPH-induced DA release, the mechanism by which L-DOPA increases extracellular DA concentration remains less well understood. In vivo microdialysis studies have demonstrated that L-DOPA increases extracellular DA in the striatum not only through an activity (i.e., action potential and Ca^{2+})-dependent process,[32−34] but also activity-independent mechanisms (e.g., after TTX[32,35−37]). In addition, L-DOPA can elevate tonic DA levels in the striatum after extensive lesion of dopaminergic terminals, as well as in other brain regions that have a lower density of dopaminergic fibers or even where such fibers are absent (e.g., cerebral cortex, hippocampus, and the cerebellum).[33,34,36−41] However, the source of this extra-nigral DA remains controversial. Serotoninergic neurons are capable of L-DOPA uptake and conversion to DA,[42,43] but L-DOPA-induced DA increase persists in the striata with depleted serotoninergic and dopaminergic innervation,[38] indicating the involvement of other types of cells including possibly nonaminergic neurons, astrocytes, and endothelial cells.[40−42,44,45] The question regarding the source of L-DOPA-derived DA remains particularly pertinent in the context of treatment of Parkinson's disease, a condition in which ~80% of nigrostriatal terminals degenerate.[46] Here, we demonstrate that FSCAV performed in brain slices can reproduce some findings previously obtained

DOI: 10.1021/acschemneuro.5b00120
ACS Chem. Neurosci. 2015, 6, 1802−1812

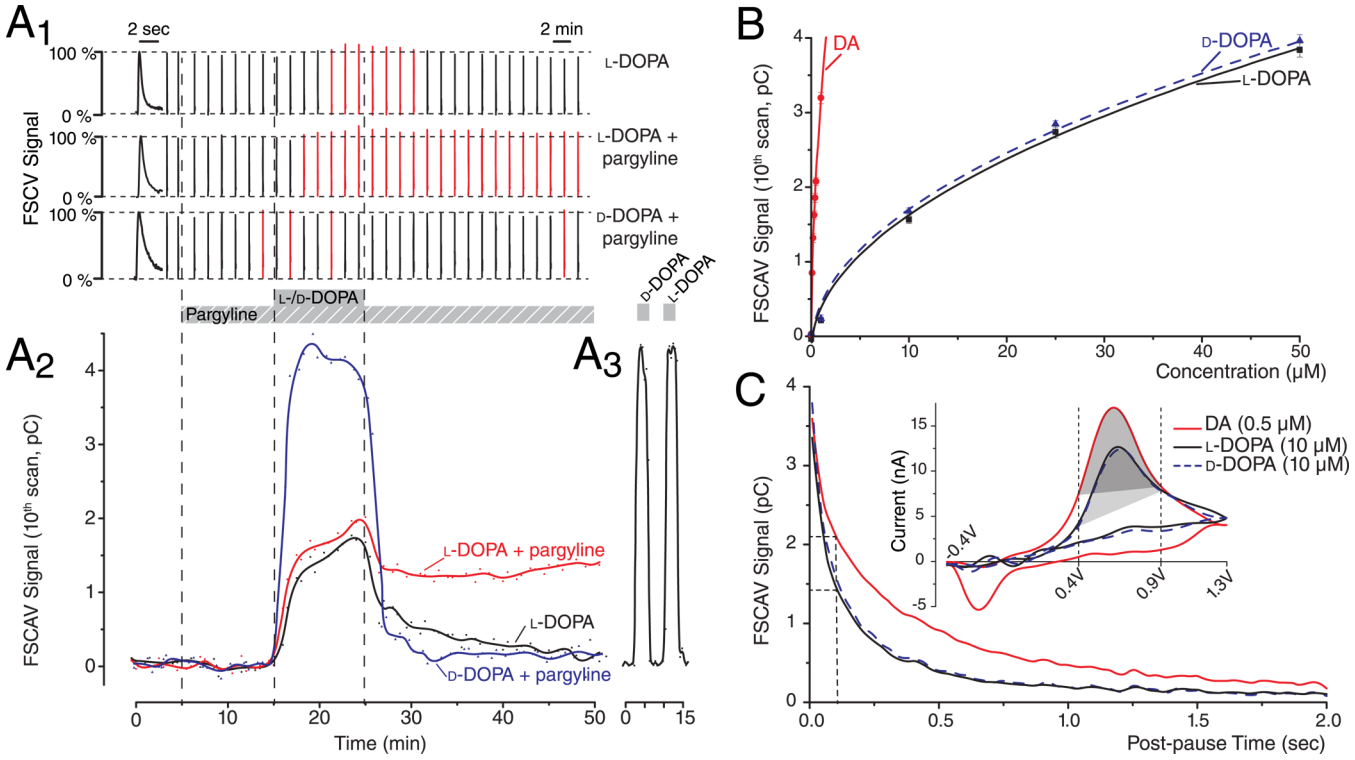

Figure 4. L-DOPA caused a long-lasting increase in tonic DA in the presence of MAO inhibition. (A) Representative examples of changes in stimulated DA release (A1) and FSCAV signal (A2) induced by L-DOPA with and without pargyline preincubation (10 μM), or D-DOPA with pargyline, all obtained with the same CFM. L-DOPA applied on its own transiently increased stimulated DA release (>100% control indicated in red, A1) and the FSCAV signal (A2); with pargyline preincubation these increases were sustained. D-DOPA did not affect electrically evoked release, but increased the FSCAV signal during application more than L-DOPA. After D-DOPA application, the FSCAV signal diminished faster than that after L-DOPA. L-DOPA and D-DOPA (3 min application each) produced the same signal when recorded outside the slice (A3). Thus, while during L-DOPA application the FSCAV signal represents contributions from L-DOPA, ≥5 min after L-DOPA washout the signal reflects tonic $[DA]_0$. (B) Example calibration of L-DOPA, D-DOPA, and DA (3 measurements at each point, single CFM). FSCAV is highly selective for DA over L-DOPA; D-DOPA is indistinguishable from L-DOPA. (C) Postpause scans increase in selectivity for DA over L-DOPA and D-DOPA. 10 μM L-DOPA or D-DOPA and 500 nM DA produced approximately equivalent FSCAV signals in the 1st postpause scans, yet due to different decay rates selectivity for DA increases with each successive scan. 10th scan (100 ms postpause; indicated) was chosen as a compromise between this improving selectivity and decreasing signal-to-noise ratio. Inset: Deconvoluted voltammograms recorded during the 10th scan after pause.

with microdialysis in vivo, offering a way of studying both the conventional (i.e., reliant on vesicular DA release from dopaminergic fibers) and unconventional (e.g., activity-independent) effects of L-DOPA in vitro.

In contrast to microdialysis approach that allows excellent (chromatographic) separation between L-DOPA and DA, in situ electrochemical detection faces a challenge to separate these two analytes due to similarity in chemical structure and thus nearly identical voltammograms. However, FSCAV markedly improves the selectivity for DA over L-DOPA when the 10th scan (rather than the 1st or 2nd) following the pause is used. This is based on the observation by Atcherley et al.[18] that, following a pause in scanning, the peak Faradaic current generated by different analytes (including DA and DA metabolites) decays to zero at various rates. In the current study, during calibration performed in beaker, 500 nM DA and 10 μM L-DOPA produced approximately the same charge as measured from the 2nd scan after the pause, but this charge decayed faster with each subsequent scan for L-DOPA than for DA. Such a difference reflects a faster rate of removal of L-DOPA from the CFM surface, likely attributable to a weaker adsorption strength of zwitterionic L-DOPA vs cationic DA, but also possibly different electron transfer kinetics and rates of mass transport.[18] When measured from the 10th scan, the DA signal was significantly greater than that resulting from L-DOPA, corresponding to a 20−200× higher (dependent on the concentrations compared and the actual CFM; n = 3 CFMs) selectivity for DA over L-DOPA on a molecule-for-molecule basis (Figure 4C). This compares favorably with only ∼10× selectivity of DA over L-DOPA in FSCV.[47]

Here, we use this greater selectivity of FSCAV for DA over L-DOPA and additional pharmacological tests to demonstrate that L-DOPA can increase tonic DA levels in slice post L-DOPA washout through an activity-independent mechanism. L-DOPA (50 μM, 10 min) increased the FSCAV signal quickly (Figure 4A2; summarized in Figure 5A2). When L-DOPA administration was stopped, the signal slowly returned to near zero (corresponding to 4.6 ± 2.4 nM DA, n = 7) over 15 min. The parallel increase in electrically stimulated DA release (139.1 ± 6.5% of control, n = 5) indicates efficient L-DOPA uptake, its conversion to DA, and vesicular storage in striatal terminals, consistent with previous reports that L-DOPA rapidly increases quantal size of released DA in cultured rat neurons, PC12 cells and chromaffin cells.[43,48] Though it is not possible to conclusively separate the changes in the FSCAV signal between the contributions of DA and L-DOPA *during* L-DOPA application, we hypothesized that because of the higher selectivity of DA over L-DOPA, the FSCAV signal recorded

DOI: 10.1021/acschemneuro.5b00120
ACS Chem. Neurosci. 2015, 6, 1802−1812

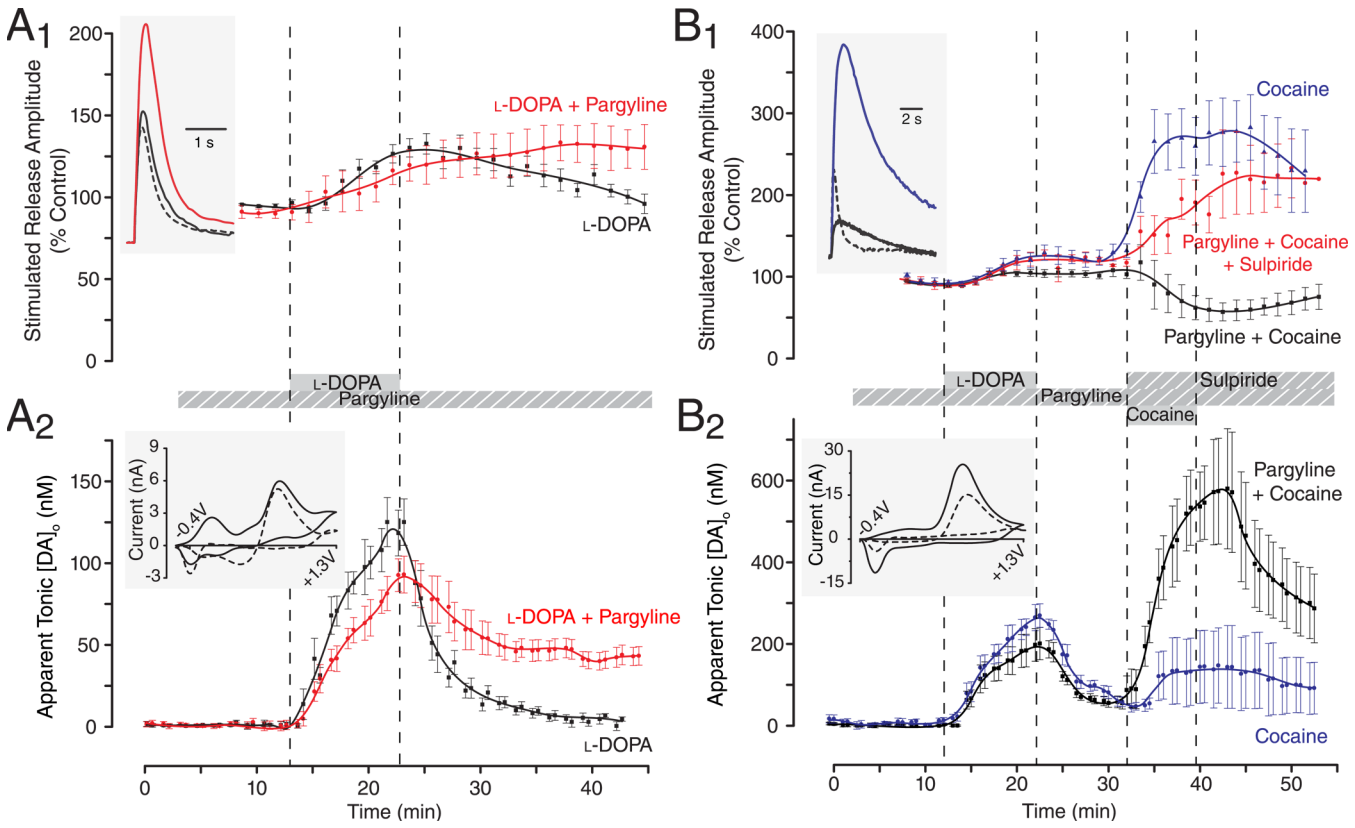

Figure 5. Effects of pharmacological blockers of MAO and DAT on L-DOPA (50 μM)-induced changes in tonic DA and stimulated release. FSCAV signal is confidently attributed to DA ≥5 min post L-DOPA washout. During L-DOPA application, *apparent* $[DA]_0$ reflects concurrent changes in L-DOPA and DA concentration that cannot be distinguished. (A) MAO inhibition with pargyline (10 μM, red; $n = 9$) resulted in sustained increases in stimulated release (A1) and tonic DA concentrations (A2), compared to L-DOPA alone which evoked transient increases (black; $n = 7$). A1 inset: Stimulated release examples (at 37 min; pre-L-DOPA control as dashed line). A2 inset: Peaks of deconvoluted voltammogram (at 37 min, in pargyline; solid line) align with stimulated release voltammogram (dashed line). (B) MAO and DAT inhibition had a synergistic effect on tonic DA. (B1) Cocaine (20 μM) increased electrically stimulated DA overflow when applied post L-DOPA washout, without pretreatment with pargyline (blue; $n = 6$). With pargyline pretreatment, cocaine inhibited stimulated DA release (black; $n = 4$). This inhibition was blocked by the D_2 antagonist sulpiride (10 μM, red; $n = 3$). (B2) Blocking DAT without MAO inhibition gave small and variable increases in the tonic DA (blue; $n = 6$). Note as tonic DA increased above 253.0 ± 49.7 nM with pargyline and cocaine, stimulated DA release decreased. B1 inset: Stimulated release (at 37 min; control; dashed line). Cocaine reduced reuptake and increased amplitude (blue), but decreased amplitude in the presence of pargyline (black). B2 inset: Deconvoluted FSCAV voltammogram (37 min, pargyline + cocaine) vs stimulated DA release (dashed line).

shortly *after* L-DOPA washout can be entirely attributed to DA. This hypothesis could not be tested by using the competitive inhibitors of aromatic L-amino acid decarboxylase (carbidopa, benserazide), as these drugs have similar chemical structures as L-DOPA and thus are also electroactive. Instead, we confirmed that the signal recorded shortly after L-DOPA washout reflects an increased DA tone in two ways: (a) the signal was strongly enhanced by inhibiting DA metabolism by monoamine oxidase (MAO); and (b) it was absent when we used D-DOPA, a stereoisomer of L-DOPA which is not efficiently converted into DA.

In the striatum, DA (including that newly synthesized from L-DOPA) is primarily metabolized by MAO in dopaminergic terminals (containing principally MAO-A) and astrocytes (containing principally MAO-B).[38] Inhibiting MAO dramatically increases the tonic DA in 6-OHDA lesioned striata as assessed with microdialysis.[38,39] Preincubation of slices in our experiments with pargyline (10 μM, nonselective MAO inhibitor) resulted in a long-lasting increase in the FSCAV signal (corresponding to 43.0 ± 5.1 nM DA 15 min post L-DOPA, $p < 0.01$, Tukey HSD posthoc test; Figure 4A2, summarized in Figure 5). MAO degrades DA (through an aldehyde intermediate) to 3,4-dihydroxyphenylacetic acid (DOPAC) and homovanilic acid (HVA). Hence, the prolonged increase in FSCAV signal during MAO inhibition confirms the signal detected post L-DOPA reflects DA, and not DA metabolites. This is consistent with our recent FSCAV study conducted in vivo, which demonstrated a pargyline-induced increase in tonic striatal DA level.[19] In addition, calibrations performed in beaker showed that the 10-th postpause FSCAV scan was more than 2 orders of magnitude more sensitive in detecting DA than DOPAC (930×) or HVA (670×). The L-DOPA-induced increase in electrically stimulated DA release measured with FSCV was percentage-wise similar in the presence and absence of MAO inhibition (129 ± 12.7% with pargyline, n = 5; Figure 5). Interestingly, in the presence of pargyline, the L-DOPA-induced increase in stimulated DA release was long lasting, parallel to the increase in tonic DA (Figure 5A). This sustained increase is likely to reflect a larger vesicular pool of DA available for stimulated release when MAO is inhibited. Since previous work demonstrated that catechol-*O*-methyltransferase (COMT) is much less important than MAO in regulating extracellular DA levels in the

DOI: 10.1021/acschemneuro.5b00120
ACS Chem. Neurosci. 2015, 6, 1802−1812

nigrostriatal pathway in rodents (though critically important in the cortex),[49] COMT inhibitors were not used.

To estimate the speed at which the contribution of L-DOPA to the FSCAV signal diminishes after L-DOPA application was stopped, a comparison was made between the effects of L-DOPA and D-DOPA. D-DOPA can be converted to L-DOPA and eventually DA through a multistep, D-amino acid oxidase and transaminase-dependent pathway, but in comparison to conversion straight from L-DOPA this process is less efficient and several orders of magnitude slower.[50] Our calibrations demonstrated that L-DOPA and D-DOPA are indistinguishable with FSCAV, with identical voltammograms, and postpause charge decays (Figure 4B, C). When D-DOPA was applied to the slice at the same concentration as L-DOPA (50 μM, 10 min), it produced a FSCAV signal approximately twice as large as that of L-DOPA (Figure 4A2), despite producing near identical signals outside the slice (Figure 4A3). This difference likely reflects the stereoselectivity of the transporters responsible for L-DOPA uptake (e.g., "System L" L-amino acid carrier[51]). Notably, the signal post D-DOPA washout returned fast to baseline (within ~5 min), even in the presence of pargyline (5.4 ± 0.8 min with pargyline, n = 4; 4.9 ± 0.3 min without, n = 4; data not shown). Assuming L-DOPA and D-DOPA diffuse in and out of slice at a similar rate, this analysis confirms that the signals recorded ≥5 min post L-DOPA application are due to DA, not L-DOPA.

2.5. The Role of DAT and VMAT2 in Prolonged Increase in Extracellular DA Following Brief L-DOPA Application. The tonic concentration of DA in the striatum is determined in vivo mainly by a balance between the activity of dopaminergic neurons and the uptake by DAT.[52] In striatal slices, there is a high abundance of DAT which may partly mask activity-independent DA-release following L-DOPA administration.[33] As expected, blocking DAT with cocaine (20 μM, 10 min; no L-DOPA application) did not increase tonic DA in slices as determined with FSCAV, consistent with a lack of electrical activity and activity-dependent DA release (n = 4, data not shown). In contrast, cocaine significantly increased tonic DA concentration after L-DOPA (Figure 5B). However, this potentiating effect was inconsistent when MAO was not inhibited with pargyline, most likely reflecting the varying amounts of extracellular DA at the time point when cocaine administration began. In the presence of pargyline, when tonic DA levels were sustained higher after L-DOPA washout, cocaine caused a significantly larger increase in tonic DA (515 ± 90.4 nM vs 137.6 ± 81.2 nM in the absence of pargyline, $p < 0.005$, n = 7 and 6 respectively). These FSCAV measurements confirm the role of DAT in limiting tonic DA concentration in the striatal slice, and indicate that, in contrast to AMPH-induced DA release (see above), reverse transport through DAT does not account for increase in tonic DA after L-DOPA (cf. ref 53). Instead, DAT activity reduces the L-DOPA-induced increase in tonic DA in slice, consistent with in vivo microdialysis data showing a smaller rise in the level of tonic DA post L-DOPA in intact vs lesioned striata.[33,34,36]

As expected, cocaine on its own, or following L-DOPA, also increased the amplitude of stimulated DA release (as measured with FSCV; Figure 5B1) by decreasing the rate of DA reuptake (Figure 5B1 inset).[54] However, when cocaine was administered after L-DOPA in the presence of pargyline, there was a large decrease in the stimulated release, correlated with the time at which tonic DA concentration increased above a certain level. As this inhibitory effect, observed in the presence of high, but not low, tonic DA levels, was largely reversed by D_2 receptor antagonist sulpiride (10 μM), it can be explained by activation of (low-affinity) D_2 autoreceptors known to reduce stimulated DA release.[55,56] The presence of the inhibitory effect of high tonic DA levels on stimulated DA release provides further evidence that the FSCAV measurements indeed tracks absolute DA concentrations. In addition, our data demonstrate that the combined FSCAV-FSCV approach, with single electrical stimuli, provides an effective functional assay for further detailed examination of D_2 autoreceptor affinity. This should have a clear advantage over previous attempts to assess D_2 autoreceptor function in brain slices which relied on pulse train stimulation[55] as, in contrast to stimulation with single pulses, DA overflow during pulse trains is also affected by other neurotransmitters.[57]

To further validate our combined FSCAV-FSCV approach, we investigated changes in tonic and stimulated DA release following inhibition of vesicular monoamine transporter 2 (VMAT2) with Ro4-1284. Inhibition of VMAT2 reduces vesicular storage and increases cytosolic DA.[29] As expected, Ro4-1284 (20 μM) sharply inhibited stimulated DA release (Figure 6A). When L-DOPA (50 μM, 10 min) was applied 20 min after the onset of Ro4-1284 application, the peak tonic DA concentration and the lag in the post L-DOPA decay were similar to the responses seen in control slices not exposed to pargyline (Figure 6B; cf. Figure 5A2). Concentrations remained elevated 15 min post L-DOPA washout, indicating the increase in tonic DA is, at least in part, independent of exocytotic

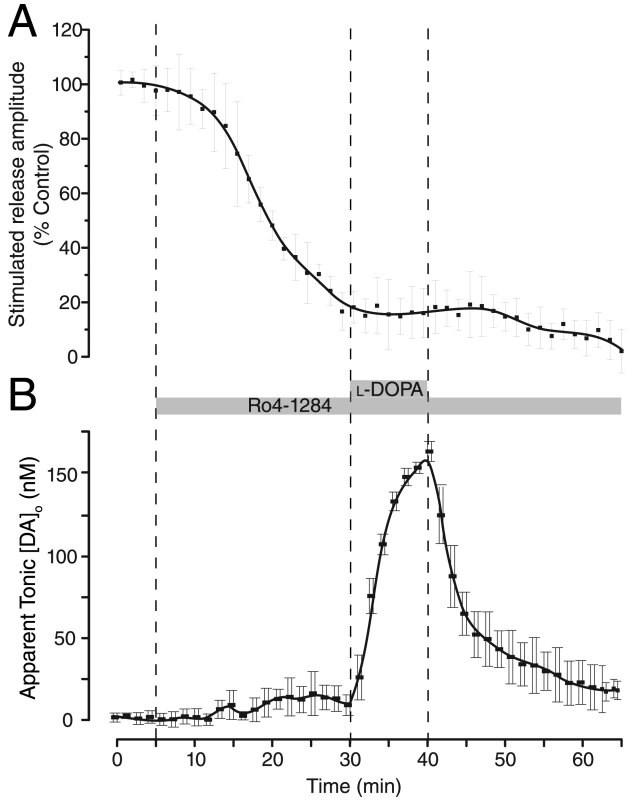

Figure 6. Combined FSCAV and FSCV recording showing the effects of VMAT2 inhibition with Ro4-1284 (20 μM) on stimulated release and tonic DA concentration before, during and after L-DOPA (50 μM, 10 min). (A) Ro4-1284 reduced stimulated release. (B) Tonic DA concentrations are sustained above baseline post L-DOPA washout (n = 5).

DOI: 10.1021/acschemneuro.5b00120
ACS Chem. Neurosci. 2015, 6, 1802−1812

release, consistent with some previous microdialysis studies.[32,33,35,37]

2.6. Summary and Conclusions. Overall, tonic DA levels measured with FSCAV responded in a predicted manner to the various pharmacological challenges used (Figures 3 and 7),

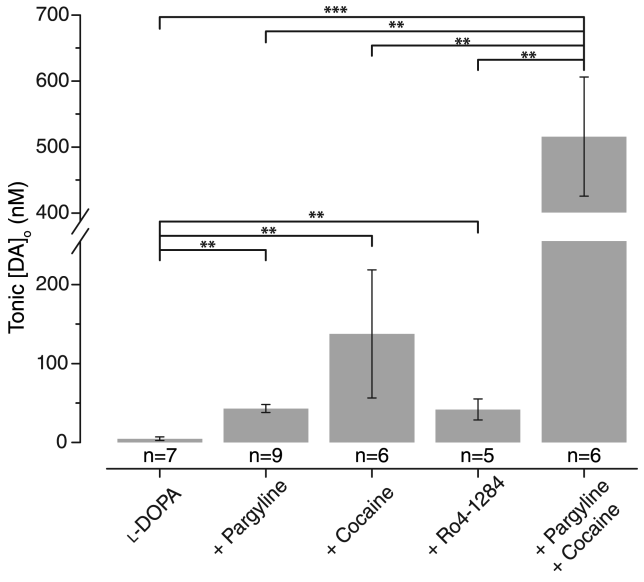

Figure 7. Summary of the effects of drugs affecting DA metabolism, uptake and storage on tonic DA concentrations recorded with FSCAV 15 min post L-DOPA washout (the time point at which L-DOPA-only recordings were not significantly different from zero, indicating that L-DOPA was not contributing to the signal). Significant effect of drug in one-way ANOVA analysis ($F_{4,29} = 25.29$, $p < 0.001$) with logarithmic correction for heteroskedasticity. Posthoc comparisons by using Tukey's HSD test (**$p < 0.01$, ***$p < 0.001$).

supporting the role of both MAO-dependent metabolism and DAT-mediated uptake in modulating tonic extracellular DA concentration not only in vivo but also in brain slice. FSCAV measurements post L-DOPA application reproduced results previously only obtainable in vivo, and demonstrates activity-independent mechanisms by which L-DOPA increases tonic DA in the healthy striatum, and not only in lesioned striata. Instability of the background current has been a major obstacle in many previous studies in which conventional FSCV recordings were used to track slow changes in concentration of electroactive substances, including DA, though FSCV has been used to follow large (>3 μM) increases in tonic DA evoked by prolonged AMPH application.[29,30] In contrast, FSCAV was used here to measure low nanomolar concentrations of DA evoked by brief AMPH application. The effects of background instability when using FSCV could be only partly remedied in previous studies by periodic subtraction of the background current using fast differential ramp voltammetry,[58,59] with reference scans generated from a baseline with an offset, resulting in pseudodifferentiation of the Faradaic current. A more successful approach is based on analogue background subtraction combined with principal component regression analysis.[60] Analog background subtraction extends FSCV measurements up to 30 min, but beyond this time the background drift is too great for analysis. In addition, this approach requires specialized hardware. In our FSCAV technique, while each pause temporarily changes the background current in each 30 s recording segment, by integrating only a narrow portion of the voltammogram there is no need for further correction. Additional drift in the background current occurring within each segment are small, and there is no requirement for the background current to be stable between consecutive segments. Therefore, FSCAV measurements are independent of slow background drifts and can continue for much longer than 30 min. Additionally, FSCAV is more sensitive than FSCV, aiding detection of nanomolar concentrations of DA or other electroactive neurotransmitters.

The other important feature of the FSCAV technique is that it allows for measurement of absolute concentration of analytes (including DA and L-DOPA), rather than only "delta" values. In addition, the problem resulting from an overlap in oxidation potential between some analytes, as faced in conventional FSCV, can be partly resolved by analysis of the 10-th scan following the pause in each FSCAV recording segment, as shown here for L-DOPA and DA. FSCAV can also be easily combined with FSCV conducted at fast scanning frequency (100 Hz), allowing for concurrent measurements of stimulated DA release (e.g., every 90 or 120 s), with greater temporal resolutions and less lag between adsorption and detection than conventional scanning at 10 Hz. Such concurrent FSCAV-FSCV measurements provide a powerful tool for investigating the complex relationship between the tonic and phasic levels of this neurotransmitter. This was illustrated in our study by showing that D_2 receptor-mediated inhibition of stimulated DA release critically depends on tonic DA levels. In FSCAV measurements we used 30 s recording segments, which resulted in 2 data points/min (or slightly less when FSCAV measurements are combined with FSCV). However, these FSCAV recording segments can be shortened to 20 s (2 s at 100 Hz, 10 s pause, 8 s at 100 Hz), resulting in a faster sampling rate (3 data points/min).

In conclusion, FSCAV can be effectively used in brain slices to measure slow changes in extracellular DA concentration expressed as absolute values, complementing studies conducted both in vivo and in vitro with other electrochemical techniques and microdialysis.

3. METHODS

3.1. Tissue Preparation. All protocols were approved by the Animal Ethics Committee of the University of Auckland in accordance with the New Zealand Government Animal Welfare Act. Following brief CO_2 anesthesia, the brain was quickly removed from P21-23 Wistar rats (n = 19) and placed in cooled (2−6 °C) carbogenated (95% O_2, 5% CO_2) artificial cerebrospinal fluid (ACSF) containing (mM): 127 NaCl, 3 KCl, $2CaCl_2$, 1.25 NaH_2PO_4, 2 $MgSO_4$, 26 $NaHCO_3$, and 10 glucose. Coronal slices (300 μm) containing the striatum were cut with a vibratome (VT1200S, Leica Biosystems). Slices were kept at 34 °C for 20 min and subsequently at room temperature. For recording, a single slice was transferred to a recording chamber (JG-23W/HP, Warner Instruments; volume ~0.6 mL) and superfused with ACSF (3.5 mL/min, 32 ± 0.5 °C) as described previously.[61,62]

3.2. Carbon-Fiber Microelectrodes (CFMs). The protocol for manufacturing cylindrical CFMs was similar to that described previously.[63] Briefly, carbon fiber (7 μm diameter, Goodfellow Cambridge Ltd.) was threaded through pulled borosilicate glass pipet (3.0 mm o.d/1.62 mm i.d., Harvard Apparatus) after breaking the tip to 10−15 μm. The section of the carbon fiber near the tip of the glass was electrically insulated and sealed by back injection of an epoxy resin (Epoxylite, Epoxylite Corp, thinned with ethyl methyl ketone; Scharlau), followed by curing overnight in an oven (120 °C). The electrode was then filled with carbon-based wire glue (Anders Products) and a copper wire with a gold-plated contact inserted. The

DOI: 10.1021/acschemneuro.5b00120
ACS Chem. Neurosci. 2015, 6, 1802−1812

fiber protruding from the tip of glass was trimmed to 50−80 μm. The Ag/AgCl reference electrode was formed by immersing silver wire in chlorine bleach. Each CFM was soaked in purified isopropyl alcohol for minimum of 10 min prior to use.[24]

3.3. Fact-Scan Controlled Adsorption Voltammetry (FSCAV). FSCAV was performed as previously described in calibration solutions and in vivo.[18,19] CFMs were positioned 100−150 μm beneath the slice surface using a micromanipulator (MP-285, Sutter Instrument Co.) in the dorsal striatum. Their potential was controlled with custom software (WCCV v.3, Knowmad Technologies, LLC) interfacing with a data-acquisition card (PCIe-6321; National Instruments) and a potientiostat (Chem-Clamp, Dagan Corporation). For FSCAV, two command voltages were generated: a triangular waveform, from −0.4 to +1.3 V (1200 V/s) repeated at 100 Hz, and a DC potential (−0.4 V). A third output via a CMOS precision analog switch (ADG419, Analogue Devices), controlled which command was relayed to the potentiostat and CFM.

After insertion into the slice, recordings were started following a short period (3−5 min) of cycling at 100 Hz (1200 V/sec) to aid electrode stabilization. Consecutive 30 s recording segments were stored to disc (~5 MB/segment; 708 data points/scan; scan duration 2.83 ms), with overall file size for recordings lasting 0.5−1.5 h ranging from 0.3 to 1.0 GB. However, data can be compressed (e.g., with 7-Zip 9.20, LMZA algorithm) to 20% of original file size for archiving.

Calibration curves of CFMs for FSCAV or FSCV recordings were obtained in a glass beaker (30 mL) filled with Tris-buffered ACSF (sodium bicarbonate/CO_2 buffer replaced with 10 mM Tris-HCl so to reduce mechanical artifacts from bubbling; glucose excluded, otherwise identical concentration of ions as standard ACSF; pH 7.4) and holding a small magnetic stir bar. The beaker was placed on a battery-operated magnetic stirrer, with CFMs dipped in the buffer. Small volumes of concentrated stock solutions of DA, L-DOPA, D-DOPA, DOPAC, or HVA were added to the buffer to obtain data for calibration.

Each pause in scanning temporarily affects the capacitive properties of the CFM and hence changes the non-Faradaic (background) current when scanning resumes. While integration method can be used for calibration (see below), for comparing FSCAV to FSCV voltammograms it was necessary to eliminate these nonspecific changes. For a given CFM, the change in background after the pause is stable and can be described by a response function obtained under control conditions (ACSF only). Inverting and applying this function, a process called deconvolution (implemented in the WCCV software), removes these nonspecific changes in the background, leaving the Faradaic currents caused by DA and/or other analytes. This is more successful than direct background subtraction, and has been previously validated in standard solutions of analytes and buffer.[18]

3.4. Concurrent FSCAV and FSCV. Concurrent measurements of electrically stimulated DA release with conventional FSCV, and absolute tonic concentrations by FSCAV, were performed in some experiments. A second data-acquisition card (PCI-6221, National Instruments) and the WCCV software interfacing with a constant-current stimulus isolation unit was used to control application of single monophasic electrical stimuli (1 ms, 25−50 μA) to a bipolar tungsten electrode placed in the vicinity of the CFM. Thirty second segments were then selected in software as either FSCV (stimulus applied, no pause in scanning) or FSCAV recordings (pause, no stimulus). This allowed FSCV recording segments to be interposed between otherwise consecutive FSCAV measurements (Figure 3A1), and assess stimulated DA release every 90 or 120 s (in 1 out of every 3 or 4 recording segments). For comparison, in some experiments, stimulated DA release was measured with constant potential amperometry (CPA), using a + 0.4 V electrode potential[25] or FSCV performed at a scan frequency of 10 Hz (1200 V/s).

3.5. Drugs. All drugs were purchased from Sigma-Aldrich, except for D-DOPA (Toronto Research Chemicals). To reduce oxidation, L-DOPA and D-DOPA were dissolved to final concentration in carbogenated ACSF immediately before use. For DA and other drugs, high concentration stock solutions (250×) were infused near the inlet of the recording chamber by computer-controlled syringe pumps (SP100i, WPI) at 1/250 of the main flow rate to achieve the final bath concentration. Sulpiride and Ro4-1284 were initially dissolved in dimethyl sulfoxide (DMSO) and then in dH_2O so that the final bath concentration of DMSO did not exceed 0.1%. All other syringe-injected drugs were prepared in dH_2O.

3.6. Analysis and Statistics. All data were filtered at 5 kHz using a zero-phase filter. For FSCAV recordings, part of the 10th voltammogram after each pause (+0.4 to +0.9 V) was integrated using WCCV software. Statistical analysis was performed in R (v3.1, R Core Team). In most cases, the integrated area (pC) was converted to a concentration (nM) using the appropriate calibration curve obtained in beaker. In FSCV recording segments, stimulated release of DA was measured as a transient change in the background-subtracted current following a single electrical pulse. Responses were normalized to three consecutive responses obtained before drug application, then averaged for comparison between different experiments. To assess the kinetics of stimulated release, a single exponential decay function was fitted between 10% and 90% amplitude. Significance was assessed at selected time points using one-way ANOVA followed by Tukey's HSD posthoc test. Graphs were prepared in OriginPro (v9.2, OriginLab). For graphical representation, the Savitzky−Golay smoothing procedure was used to interpolate between individual measurements. Data are presented as mean ± SEM (unless stated otherwise), with $p < 0.05$ considered significant.

AUTHOR INFORMATION

Corresponding Author

*E-mail: j.lipski@auckland.ac.nz. Phone: +64-99236737.

Present Address

§C.W.A.: Department of Research, Mayo Clinic, Scottsdale, AZ 85259, USA.

Author Contributions

M.H.B. and J.L. designed experiments. M.H.B. performed experiments and analyzed data. C.W.A. and M.L.H. provided software and advice, and contributed to analysis. M.H.B. and J.L. interpreted the data and wrote the manuscript. All authors edited and approved the final manuscript.

Funding

The study was supported by the Auckland Medical Research Foundation (J.L.; 9134/3703809) and NIH (M.L.H.; DA035425)

Notes

The authors declare the following competing financial interest(s): C.W.A. and M.L.H. co-own Knowmad LLC., which develops and markets the WCCV software used here. M.H.B. and J.L. declare no competing financial interest.

ACKNOWLEDGMENTS

The authors thank Justine Fuller and Brian Hyland (University of Otago, N.Z.) for the protocol and help with production of CFMs, and Jordan T. Yorgason (Oregon Health and Science Centre, Vollum Institute) for helpful discussions.

ABBREVIATIONS

ACSF, artificial cerebrospinal fluid; AMPH, amphetamine; CFM, carbon fiber microelectrode; COMT, catechol-*O*-methyltransferase; CPA, constant potential amperometry; D-DOPA, D-3,4-dihydroxyphenylalanine; DA, dopamine; DAT, dopamine transporter; DOPAC, 3,4-dihydroxyphenylacetic acid; FSCV, fast-scan cyclic voltammetry; FSCAV, fast-scan controlled-adsorption voltammetry; HVA, homovanilic acid; L-DOPA, L-3,4-dihydroxyphenylalanine; MAO, monoamine oxidase; Ro4-1284, 2-hydroxy-2-ethyl-3-isobutyl-9,10-dime-

DOI: 10.1021/acschemneuro.5b00120
ACS Chem. Neurosci. 2015, 6, 1802−1812

thoxy-1,2,3,4,5,6,7-hexahydrobenzo[a]chinolizine; VMAT2, vesicular monoamine transport 2

REFERENCES

(1) Arbuthnott, G. W., and Wickens, J. (2007) Space, time and dopamine. *Trends Neurosci. 30*, 62−69.

(2) Grace, A. A., Floresco, S. B., Goto, Y., and Lodge, D. J. (2007) Regulation of firing of dopaminergic neurons and control of goal-directed behaviors. *Trends Neurosci. 30*, 220−227.

(3) Schultz, W. (2007) Multiple dopamine functions at different time courses. *Annu. Rev. Neurosci. 30*, 259−288.

(4) Bull, D. R., Palij, P., Sheehan, M. J., Millar, J., Stamford, J. A., Kruk, Z. L., and Humphrey, P. P. (1990) Application of fast cyclic voltammetry to measurement of electrically evoked dopamine overflow from brain slices in vitro. *J. Neurosci. Methods 32*, 37−44.

(5) Patel, J. C., and Rice, M. E. (2013) Monitoring axonal and somatodendritic dopamine release using fast-scan cyclic voltammetry in brain slices. *Methods Mol. Biol. 964*, 243−273.

(6) Robinson, D. L., Hermans, A., Seipel, A. T., and Wightman, R. M. (2008) Monitoring rapid chemical communication in the brain. *Chem. Rev. 108*, 2554−2584.

(7) Robinson, D. L., Venton, B. J., Heien, M. L., and Wightman, R. M. (2003) Detecting subsecond dopamine release with fast-scan cyclic voltammetry in vivo. *Clin. Chem. 49*, 1763−1773.

(8) Heien, M. L., Khan, A. S., Ariansen, J. L., Cheer, J. F., Phillips, P. E., Wassum, K. M., and Wightman, R. M. (2005) Real-time measurement of dopamine fluctuations after cocaine in the brain of behaving rats. *Proc. Natl. Acad. Sci. U. S. A. 102*, 10023−10028.

(9) Chen, K. C. (2006) The validity of intracerebral microdialysis, In *Handbook of Behavioral Neuroscience* (Ben, H. C. W., and Thomas, I. F. H. C., Eds.), pp 47−70, Chapter 1.4 , Elsevier, Amsterdam.

(10) Myers, R. D., Adell, A., and Lankford, M. F. (1998) Simultaneous comparison of cerebral dialysis and push-pull perfusion in the brain of rats: a critical review. *Neurosci. Biobehav. Rev. 22*, 371−387.

(11) Young, A. M. (1993) Intracerebral microdialysis in the study of physiology and behaviour. *Rev. Neurosci. 4*, 373−395.

(12) Dingledine, R. (1984) *Brain slices*, Plenum Press, New York.

(13) Geffen, L. B., Jessell, T. M., Cuello, A. C., and Iversen, L. L. (1976) Release of dopamine from dendrites in rat substantia nigra. *Nature 260*, 258−260.

(14) Goshima, Y., Kubo, T., and Misu, Y. (1988) Transmitter-like release of endogenous 3,4-dihydroxyphenylalanine from rat striatal slices. *J. Neurochem. 50*, 1725−1730.

(15) Russell, V. A., Lamm, M. C., and Taljaard, J. J. (1988) Effect of ethanol on [3H]dopamine release in rat nucleus accumbens and striatal slices. *Neurochem. Res. 13*, 487−492.

(16) Aliaga, E., Bustos, G., and Gysling, K. (1995) Release of endogenous catecholamines from the striatum and bed nucleus of stria terminalis evoked by potassium and N-methyl-D-aspartate: in vitro microdialysis studies. *J. Neurosci. Res. 40*, 89−98.

(17) Bradberry, C. W., Sprouse, J. S., Sheldon, P. W., Aghajanian, G. K., and Roth, R. H. (1991) In vitro microdialysis: a novel technique for stimulated neurotransmitter release measurements. *J. Neurosci. Methods 36*, 85−90.

(18) Atcherley, C. W., Laude, N. D., Parent, K. L., and Heien, M. L. (2013) Fast-scan controlled-adsorption voltammetry for the quantification of absolute concentrations and adsorption dynamics. *Langmuir 29*, 14885−14892.

(19) Atcherley, C. W., Wood, K. M., Parent, K. L., Hashemi, P., and Heien, M. L. (2015) The coaction of tonic and phasic dopamine dynamics. *Chem. Commun. (Cambridge, U. K.) 51*, 2235−2238.

(20) Jones, S. R., Garris, P. A., Kilts, C. D., and Wightman, R. M. (1995) Comparison of dopamine uptake in the basolateral amygdaloid nucleus, caudate-putamen, and nucleus accumbens of the rat. *J. Neurochem. 64*, 2581−2589.

(21) Kelly, R. S., and Wightman, R. M. (1987) Detection of dopamine overflow and diffusion with voltammetry in slices of rat brain. *Brain Res. 423*, 79−87.

(22) Ferris, M. J., Espana, R. A., Locke, J. L., Konstantopoulos, J. K., Rose, J. H., Chen, R., and Jones, S. R. (2014) Dopamine transporters govern diurnal variation in extracellular dopamine tone. *Proc. Natl. Acad. Sci. U. S. A. 111*, E2751−2759.

(23) MacGregor, D. G., Chesler, M., and Rice, M. E. (2001) HEPES prevents edema in rat brain slices. *Neurosci. Lett. 303*, 141−144.

(24) Bath, B. D., Michael, D. J., Trafton, B. J., Joseph, J. D., Runnels, P. L., and Wightman, R. M. (2000) Subsecond adsorption and desorption of dopamine at carbon-fiber microelectrodes. *Anal. Chem. 72*, 5994−6002.

(25) Kile, B. M., Walsh, P. L., McElligott, Z. A., Bucher, E. S., Guillot, T. S., Salahpour, A., Caron, M. G., and Wightman, R. M. (2012) Optimizing the Temporal Resolution of Fast-Scan Cyclic Voltammetry. *ACS Chem. Neurosci. 3*, 285−292.

(26) Venton, B. J., Troyer, K. P., and Wightman, R. M. (2002) Response times of carbon fiber microelectrodes to dynamic changes in catecholamine concentration. *Anal. Chem. 74*, 539−546.

(27) Atcherley, C. W., Laude, N. D., Monroe, E. B., Wood, K. M., Hashemi, P., and Heien, M. L. (2014) Improved Calibration of Voltammetric Sensors for Studying Pharmacological Effects on Dopamine Transporter Kinetics in Vivo. *ACS Chem. Neurosci.*, 1509−1516.

(28) Leviel, V. (2011) Dopamine release mediated by the dopamine transporter, facts and consequences. *J. Neurochem. 118*, 475−489.

(29) Jones, S. R., Gainetdinov, R. R., Wightman, R. M., and Caron, M. G. (1998) Mechanisms of amphetamine action revealed in mice lacking the dopamine transporter. *J. Neurosci. 18*, 1979−1986.

(30) Schmitz, Y., Lee, C. J., Schmauss, C., Gonon, F., and Sulzer, D. (2001) Amphetamine distorts stimulation-dependent dopamine overflow: Effects on D2 autoreceptors, transporters, and synaptic vesicle stores. *J. Neurosci. 21*, 5916−5924.

(31) Siciliano, C. A., Calipari, E. S., Ferris, M. J., and Jones, S. R. (2014) Biphasic mechanisms of amphetamine action at the dopamine terminal. *J. Neurosci. 34*, 5575−5582.

(32) Rodriguez, M., Morales, I., Gonzalez-Mora, J. L., Gomez, I., Sabate, M., Dopico, J. G., Rodriguez-Oroz, M. C., and Obeso, J. A. (2007) Different levodopa actions on the extracellular dopamine pools in the rat striatum. *Synapse 61*, 61−71.

(33) Miller, D. W., and Abercrombie, E. D. (1999) Role of high-affinity dopamine uptake and impulse activity in the appearance of extracellular dopamine in striatum after administration of exogenous L-DOPA: studies in intact and 6-hydroxydopamine-treated rats. *J. Neurochem. 72*, 1516−1522.

(34) Maeda, T., Kannari, K., Suda, T., and Matsunaga, M. (1999) Loss of regulation by presynaptic dopamine D2 receptors of exogenous L-DOPA-derived dopamine release in the dopaminergic denervated striatum. *Brain Res. 817*, 185−191.

(35) Mizoguchi, K., Yokoo, H., Yoshida, M., Tanaka, T., and Tanaka, M. (1993) Dopamine formation from L-dopa administered exogenously is independent of dopaminergic neuronal activity: studies with in vivo microdialysis. *Brain Res. 611*, 152−154.

(36) Sarre, S., De Klippel, N., Herregodts, P., Ebinger, G., and Michotte, Y. (1994) Biotransformation of locally applied L-dopa in the corpus striatum of the hemi-parkinsonian rat studied with microdialysis. *Naunyn-Schmiedeberg's Arch. Pharmacol. 350*, 15−21.

(37) Abercrombie, E. D., and Zigmond, M. J. (1991) In Vivo Neurochemical Analyses of Exogenously Administered L-DOPA: Implications for Treatment of Parkinson's Disease. In *The Basal Ganglia III* (Bernardi, G., Carpenter, M., Di Chiara, G., Morelli, M., and Stanzione, P., Eds.), pp 673−682, Springer: New York.

(38) Sader-Mazbar, O., Loboda, Y., Rabey, M. J., and Finberg, J. P. (2013) Increased L-DOPA-derived dopamine following selective MAO-A or -B inhibition in rat striatum depleted of dopaminergic and serotonergic innervation. *Br. J. Pharmacol. 170*, 999−1013.

(39) Wachtel, S. R., and Abercrombie, E. D. (1994) L-3,4-dihydroxyphenylalanine-induced dopamine release in the striatum of intact and 6-hydroxydopamine-treated rats: differential effects of monoamine oxidase A and B inhibitors. *J. Neurochem. 63*, 108−117.

DOI: 10.1021/acschemneuro.5b00120
ACS Chem. Neurosci. 2015, 6, 1802−1812

(40) Navailles, S., Lagiere, M., Contini, A., and De Deurwaerdere, P. (2013) Multisite intracerebral microdialysis to study the mechanism of L-DOPA induced dopamine and serotonin release in the parkinsonian brain. *ACS Chem. Neurosci. 4*, 680−692.
(41) Hefti, F., Melamed, E., and Wurtman, R. J. (1981) The site of dopamine formation in rat striatum after L-DOPA administration. *J. Pharmacol. Exp. Ther. 217*, 189−197.
(42) Lindgren, H. S., Andersson, D. R., Lagerkvist, S., Nissbrandt, H., and Cenci, M. A. (2010) L-DOPA-induced dopamine efflux in the striatum and the substantia nigra in a rat model of Parkinson's disease: temporal and quantitative relationship to the expression of dyskinesia. *J. Neurochem. 112*, 1465−1476.
(43) Mosharov, E. V., Borgkvist, A., and Sulzer, D. (2015) Presynaptic effects of levodopa and their possible role in dyskinesia. *Mov. Disord. 30*, 45−53.
(44) Melamed, E., Hefti, F., and Wurtman, R. J. (1980) Non-aminergic striatal neurons convert exogenous L-dopa to dopamine in parkinsonism. *Ann. Neurol. 8*, 558−563.
(45) Lloyd, K., and Hornykiewicz, O. (1970) Parkinson's disease: activity of L-dopa decarboxylase in discrete brain regions. *Science 170*, 1212−1213.
(46) Bernheimer, H., Birkmayer, W., Hornykiewicz, O., Jellinger, K., and Seitelberger, F. (1973) Brain dopamine and the syndromes of Parkinson and Huntington. Clinical, morphological and neurochemical correlations. *J. Neurol. Sci. 20*, 415−455.
(47) Mosharov, E. V., Gong, L. W., Khanna, B., Sulzer, D., and Lindau, M. (2003) Intracellular patch electrochemistry: regulation of cytosolic catecholamines in chromaffin cells. *J. Neurosci. 23*, 5835−5845.
(48) Pothos, E., Desmond, M., and Sulzer, D. (1996) L-3,4-dihydroxyphenylalanine increases the quantal size of exocytotic dopamine release in vitro. *J. Neurochem. 66*, 629−636.
(49) Mercuri, N. B., Federici, M., and Bernardi, G. (1999) Inhibition of catechol-O-methyltransferase (COMT) in the brain does not affect the action of dopamine and levodopa: an in vitro electrophysiological evidence from rat mesencephalic dopamine neurons. *J. Neural Transm. 106*, 1135−1140.
(50) Kawazoe, T., Tsuge, H., Imagawa, T., Aki, K., Kuramitsu, S., and Fukui, K. (2007) Structural basis of D-DOPA oxidation by D-amino acid oxidase: alternative pathway for dopamine biosynthesis. *Biochem. Biophys. Res. Commun. 355*, 385−391.
(51) Sebastianelli, L., Ledonne, A., Marrone, M. C., Bernardi, G., and Mercuri, N. B. (2008) The L-amino acid carrier inhibitor 2-aminobicyclo[2.2.1]heptane-2-carboxylic acid (BCH) reduces L-dopa-elicited responses in dopaminergic neurons of the substantia nigra pars compacta. *Exp. Neurol. 212*, 230−233.
(52) Owesson-White, C. A., Roitman, M. F., Sombers, L. A., Belle, A. M., Keithley, R. B., Peele, J. L., Carelli, R. M., and Wightman, R. M. (2012) Sources contributing to the average extracellular concentration of dopamine in the nucleus accumbens. *J. Neurochem. 121*, 252−262.
(53) Mercuri, N. B., Calabresi, P., and Bernardi, G. (1991) Dopamine uptake inhibition potentiates the effects of L-DOPA on rat substantia nigra zona compacta neurons. *Neurosci. Lett. 126*, 79−82.
(54) Yorgason, J. T., Espana, R. A., and Jones, S. R. (2011) Demon voltammetry and analysis software: analysis of cocaine-induced alterations in dopamine signaling using multiple kinetic measures. *J. Neurosci. Methods 202*, 158−164.
(55) Cragg, S. J., and Greenfield, S. A. (1997) Differential autoreceptor control of somatodendritic and axon terminal dopamine release in substantia nigra, ventral tegmental area, and striatum. *J. Neurosci. 17*, 5738−5746.
(56) Ford, C. P. (2014) The role of D2-autoreceptors in regulating dopamine neuron activity and transmission. *Neuroscience 282*, 13−22.
(57) Rice, M. E., Patel, J. C., and Cragg, S. J. (2011) Dopamine release in the basal ganglia. *Neuroscience 198*, 112−137.
(58) Hosford, P. S., Millar, J., and Ramage, A. G. (2015) Cardiovascular afferents cause the release of 5-HT in the nucleus tractus solitarii; this release is regulated by the low- (PMAT) not the high-affinity transporter (SERT). *J. Physiol. 593*, 1715−1729.
(59) Millar, J., and Williams, G. V. (1991) Fast differential ramp voltammetry: a new voltammetric technique designed specifically for use in neuronal tissue. *J. Electroanal. Chem. Interfacial Electrochem. 282*, 33−49.
(60) Hermans, A., Keithley, R. B., Kita, J. M., Sombers, L. A., and Wightman, R. M. (2008) Dopamine detection with fast-scan cyclic voltammetry used with analog background subtraction. *Anal. Chem. 80*, 4040−4048.
(61) Guatteo, E., Yee, A., McKearney, J., Cucchiaroni, M. L., Armogida, M., Berretta, N., Mercuri, N. B., and Lipski, J. (2013) Dual effects of L-DOPA on nigral dopaminergic neurons. *Exp. Neurol. 247*, 582−594.
(62) Yee, A. G., Lee, S. M., Hunter, M. R., Glass, M., Freestone, P. S., and Lipski, J. (2014) Effects of the Parkinsonian toxin MPP+ on electrophysiological properties of nigral dopaminergic neurons. *NeuroToxicology 45*, 1−11.
(63) Ponchon, J. L., Cespuglio, R., Gonon, F., Jouvet, M., and Pujol, J. F. (1979) Normal pulse polarography with carbon fiber electrodes for in vitro and in vivo determination of catecholamines. *Anal. Chem. 51*, 1483−1486.

DOI: 10.1021/acschemneuro.5b00120
ACS Chem. Neurosci. 2015, 6, 1802−1812